Chemical doping and high-pressure studies of layered β-$PdBi_2$ single crystals

Kui Zhao,[1] Bing Lv,[1,*] Yu-Yi Xue,[1] Xi-Yu Zhu,[1,2] L. Z. Deng,[1] Zheng Wu,[1] and C. W. Chu[1,3]

[1]*Texas Center for Superconductivity and Department of Physics, University of Houston, Houston, Texas 77204-5002, USA*

[2]*Department of Physics, Nanjing University, Nanjing, China*

[3]*Lawrence Berkeley National Laboratory, Berkeley, California 94720, USA*

(Received 18 June 2015; revised manuscript received 15 August 2015; published 4 November 2015)

We have systematically grown large single crystals of the layered compounds β-$PdBi_2$, and both the hole-doped $PdBi_{2-x}Pb_x$ and the electron-doped Na_xPdBi_2, and studied their magnetic and transport properties. Hall effect measurements on $PdBi_2$, $PdBi_{1.8}Pb_{0.2}$, and $Na_{0.057}PdBi_2$ show that the charge transport is dominated by electrons in all of the samples. The electron concentration is substantially reduced upon Pb doping in $PdBi_{2-x}Pb_x$ and increased upon Na intercalation in Na_xPdBi_2, indicating effective hole doping by Pb and electron doping by Na. We observed a monotonic decrease of the superconducting transition temperature (T_c) from 5.4 K in undoped $PdBi_2$ to less than 2 K for $x > 0.35$ in hole-doped $PdBi_{2-x}Pb_x$. Meanwhile, a rapid decrease of T_c with Na intercalation is also observed in the electron-doped Na_xPdBi_2, which is in disagreement with the theoretical expectation. In addition, both the magnetoresistance and Hall resistance further reveal evidence for a possible spin excitation associated with Fermi surface reconstruction at ~50 K in the Na-intercalated $PdBi_2$ sample. The complete phase diagram is thus established from hole doping to electron doping. Meanwhile, a high-pressure study of the undoped $PdBi_2$ shows that the T_c is linearly suppressed under pressure with a dT_c/dP coefficient of -0.28 K/GPa.

DOI: 10.1103/PhysRevB.92.174404 PACS number(s): 74.25.−q, 74.62.−c, 74.70.Ad

I. INTRODUCTION

Low-dimensional compounds, with simple structure building motifs and weak bonding force between layers, have generated much research interest within condensed matter physics over the past several decades. These low-dimensional materials have displayed a variety of unusual physical phenomena such as charge density waves in transition metal chalcogenides [1,2]; spin density waves in the parent Fe pnictide superconductors [3,4]; topological order in Bi_2Se_3 [5,6]; and superconductivity in many compounds such as MgB_2 [7], doped ZrNCl [8], etc. In the binary Pd-Bi alloy family, several phases with different structures have been studied in the past [9]; in this family the $PdBi_2$ is found to crystallize in two different layered structures with a low-temperature α phase below 380 °C and a high-temperature β phase between 380 and 490 °C [10]. The α-$PdBi_2$ crystallizes in a layered monoclinic ($c2/m$) structure with a six-coordinated $PdBi_6$ building motif, while the β-$PdBi_2$ forms a layered tetragonal $CuZr_2$-type structure ($I4/mmm$) with an eight-coordinated $PdBi_8$ building motif. Every four Bi atoms in β-$PdBi_2$ are face shared with the neighboring CsCl-type $PdBi_8$ motif and therefore form a $PdBi_{8/4} = PdBi_2$ layer. The resulting $PdBi_2$ layers are packed alternately and form the body-centered tetragonal structure, as shown in the inset of Fig. 1(a). The interlayer spacing between the alternating $PdBi_2$ layers is rather large, with interlayer Bi-Bi distance of ~3.8 Å, indicating that there is no effective bonding between those layers. Various phases in the Pb-Bi system have been identified as superconductors [11], such as α-PdBi with $T_c \sim 3.8$ K, α-$PdBi_2$ with $T_c \sim 1.73$ K, β-$PdBi_2$ with $T_c \sim 4.25$ K, and $Pd_{2.5}Bi_{1.5}$ with $T_c \sim 3.7$–4 K. Early studies showed that β-$PdBi_2$ had the highest T_c among these phases, 4.25 K [11], and it was recently shown that the T_c could be further raised to 5.4 K by improving the sample quality [12]. However, neither the details of the chemical doping nor the high-pressure effect are well known in β-$PdBi_2$. The prior specific heat and STM studies on β-$PdBi_2$ suggest that it is a multiband superconductor [12,13], which is in agreement with the results from first-principles calculations [14]. Theoretical calculation shows that the density of states (DOS) around the Fermi level is dominated by the Pd $4d$ and Bi $6p$ states, and that the Fermi level is located on a positive slope below a DOS peak. Therefore, hole doping is expected to shift the Fermi level away from the DOS peak, resulting in a decrease of the DOS at the Fermi level, while electron doping will increase it. Thus one would expect a decrease of T_c upon hole doping and an increase of T_c under electron doping. Under this motivation, we decided to carry out systematic hole doping (substitution of Bi with Pb) and electron doping (Na intercalation) studies on the β-$PdBi_2$ system. However, we found that the T_c was suppressed in both cases, the reasons for which will be discussed in this paper. Meanwhile, a high-pressure study was also carried out on the β-$PdBi_2$ single crystal, and we observed a suppression of T_c upon applying pressure with a dT_c/dP coefficient of -0.28 K/GPa. The phase diagrams, both upon chemical doping and under high pressure, are presented.

II. EXPERIMENTAL DETAILS

The β-$PdBi_2$ single crystals were synthesized through a melt-growth method. Stoichiometric amounts of Pd and Bi grains were sealed in an evacuated quartz tube, which was heated up to 700 °C, kept for 10 h, and then slowly cooled to 450°C over 30 h. In order to retain the β phase, the tube was then quenched in iced water directly from 450 °C. Similarly, it was attempted to grow a series of $PdBi_{2-x}Pb_x$ ($x = 0.0$, 0.08, 0.15, 0.20, 0.28, 0.35, 0.40 0.60, 0.80, and

*Present address: Department of Physics, University of Texas at Dallas, Richardson, TX 75080; blv@utdallas.edu

 ©2015 American Physical Society

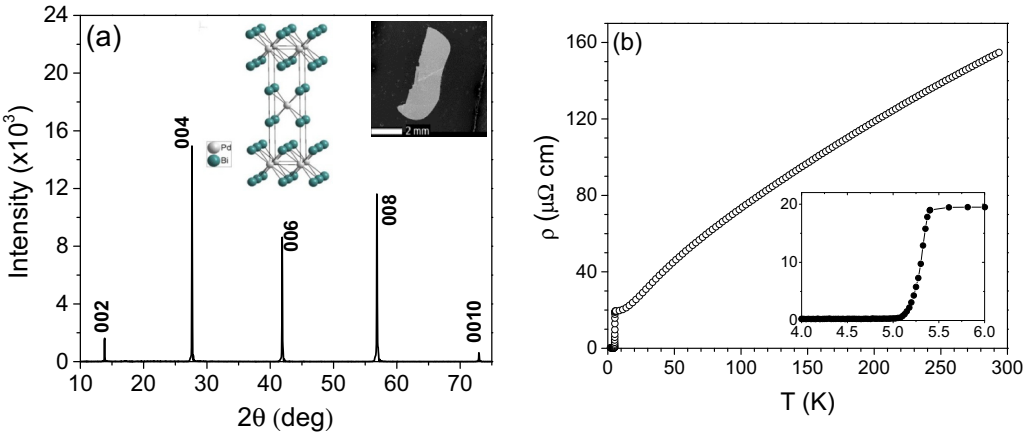

FIG. 1. (Color online) (a) XRD pattern of β-$PdBi_2$ with preferred orientation along c axis; the inset shows the crystal structure and one representative crystal SEM image. (b) Resistivity of β-$PdBi_2$ from 2 to 300 K; the inset displays resistivity data between 4 and 6 K.

1.0) crystals with stoichiometric amounts of Pd, Bi, and Pb. In addition, the Na_xPdBi_2 compounds were grown by mixing Na and the previously obtained $PdBi_2$ precursor, followed by the same synthetic conditions but using a carbon-coated quartz tube to prevent the possible reaction of sodium with the quartz tube at high temperature. The carbon coating of the quartz tube was found to be intact after the synthesis, indicating the success of the growth. X-ray powder diffraction was performed on the powdered Pb-doped single crystals at room temperature from 10° to 90° using a Panalytical X'pert diffractometer. The actual chemical compositions were determined by wavelength-dispersive spectrometry (WDS) on a JEOL JXA-8600 electron microprobe analyzer. At least six well-separated points across the crystal were measured to confirm the homogeneity of the dopants. The dc magnetic susceptibility was measured as a function of temperature, $\chi(T)$, using a Quantum Design magnetic property measurement system (MPMS) down to 2 K. Electrical resistivity as a function of temperature, $\rho(T)$, and field, $\rho(H)$, was measured by employing a standard four-probe method using a Linear Research LR400 ac bridge operated at 15.9 Hz in a Quantum Design physical property measurement system (PPMS) up to 7 T and down to 1.9 K. High-pressure resistivity measurements with a four-lead technique using the LR-400 resistance bridge were made in a Be-Cu pressure cell using Fluorinert FC77 as the pressure medium. A lead manometer was used to measure the pressure *in situ* with the LR400 inductance bridge [15]. The Hall resistivity measurements were performed in the PPMS system with fields up to 5 T using the five-lead technique, which balanced the longitudinal resistance at close to zero.

III. RESULTS AND DISCUSSION

β-$PdBi_2$ single crystals with shining metallic luster, typical size of 5 mm, and preferred orientation along the c axis after cleavage, could be obtained through the melt-growth technique, as shown in Fig. 1(a). The calculated lattice parameter c [12.963(3) Å] is consistent with previous reports [12]. A representative SEM image of the undoped β-$PdBi_2$ single crystal is also shown as the inset of Fig. 1(a). Both resistivity and magnetization measurements have shown that the superconducting transition temperature of the as-grown β-$PdBi_2$ crystal is 5.4 K, indicating the improved quality of the grown crystals as also pointed out by previous reports [12]. The resistivity curve exhibits a hump below 150 K and a minor downturn around 50 K, as shown in Fig. 1(b), suggesting possible strong electron/spin correlation in this compound.

Figure 2 shows the powder x-ray diffraction (XRD) patterns with Miller indices of the crushed crystals for the Pb-doped $PdBi_{2-x}Pb_x$ ($x = 0.08$, 0.15, 0.20, 0.28 0.35, and 0.40) samples. Except for a few minor peaks of the α phase present at low doping level, namely, $x = 0.08$, all of the peaks are well indexed into the β-$PdBi_2$-type body-centered tetragonal structures in all of the samples with different doping levels. These crystals are quite stable outside the glovebox for several months. Due to the close radius sizes between Pb and Bi, the change of lattice parameter upon Pb doping is very small, and a gradual decrease of the lattice parameter from 12.963(3) Å for $x = 0$ to 12.940(2) Å for $x = 0.4$ is observed, but the

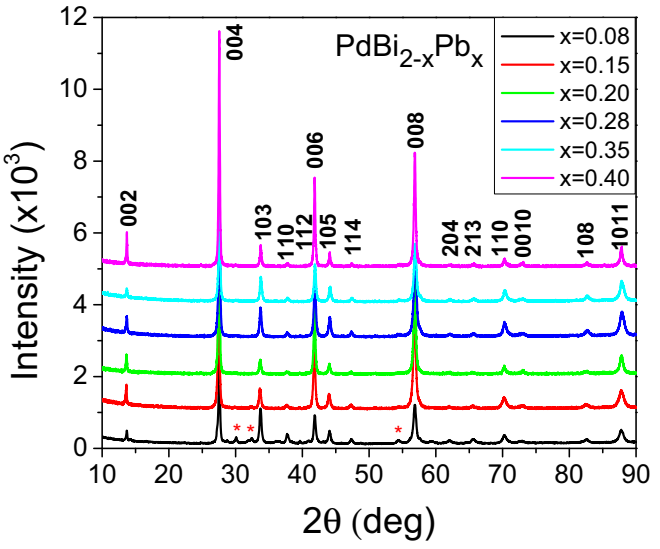

FIG. 2. (Color online) The powder x-ray diffraction patterns of $PdBi_{2-x}Pb_x$ with Miller indices. The patterns are vertically offset for better clarity. Some minor impurity peaks from the α phase are marked as *.

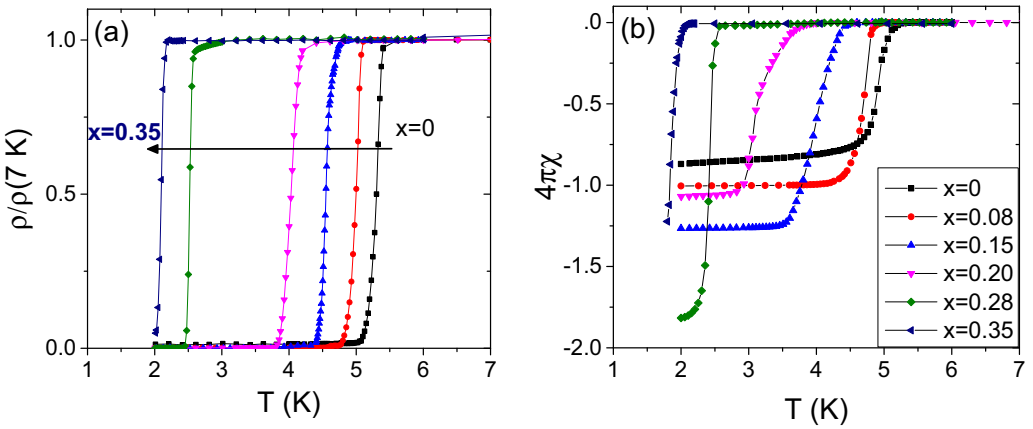

FIG. 3. (Color online) The resistivity (a) and magnetic susceptibility (b) data under $H = 2$ Oe of $PdBi_{2-x}Pb_x$ with $x = 0$–0.35 from 2 to 7 K.

overall lattice parameter change is less than 0.2%. To further confirm the homogeneity of the doped samples and establish the actual doping levels, we performed chemical analyses through WDS measurements on the single crystals. The Pb concentration is homogeneous throughout the whole sample in all cases, indicating the formation of solid solutions for these Pb-doped samples. The actual Pb-doping levels are $x = 0.08(2)$, 0.14(2), 0.19(2), 0.27(2), 0.34(1), and 0.39(1), for the nominal compositions of $x = 0.08$, 0.15, 0.20, 0.28, 0.35, and 0.40 in $PdBi_{2-x}Pb_x$, respectively. The results show that the actual doping levels are very close to the nominal compositions. Some extra impurity peaks belonging to the α-$PdBi_2$ monoclinic phase emerge at the doping level $x = 0.60$ from x-ray powder diffraction measurements and become more dominant with further Pb doping. At the doping level of $x = 1.00$, the XRD pattern shows a nearly pure phase of the α-$PdBi_2$-type structure with no detectable β phase, implying the solubility limit of the tetragonal β-$PdBi_{2-x}Pb_x$ phase at this high doping level.

Systematic resistivity and magnetization measurements were carried out for all samples with different doping levels. As shown in Fig. 3(a), the superconducting transition temperature T_c of $PdBi_{2-x}Pb_x$ continuously decreases upon Pb substitution, from 5.4 K for $x = 0$, to 4.9 K for $x = 0.08$, 4.4 K for $x = 0.15$, 3.8 K for $x = 0.20$, 2.5 K for $x = 0.28$, and 2.2 K for $x = 0.35$. The sample eventually becomes nonsuperconducting above 2 K when the doping level reaches $x = 0.40$. The superconducting transition width (10%–90% resistivity drop) is rather narrow (less than 0.3 K) in all samples, indicating the good quality of the doped samples.

Similar consistent results were obtained through magnetic susceptibility measurements as shown in Fig. 3(b). The magnetization was measured under an applied magnetic field of 2 Oe on randomly oriented small crystals with typical mass ~20 mg packed in gelatin capsules. All of the samples with doping level $0 < x < 0.35$ exhibit substantial diamagnetic shifts at the lowest temperature. The shielding fractions $4\pi\chi$ are close to or exceed 1 without the demagnetization factor correction, which implies the bulk superconducting nature of these samples. Consistent with the resistivity data, the superconducting transition temperature systematically moves downward with doping from 5.2 K for $x = 0$ to 2 K for $x = 0.40$.

To confirm the effective hole doping by Pb substitution, Hall effect measurements have been carried out to evaluate the charge carrier concentration for the parent compound $PdBi_2$ and a representative Pb-doped $PdBi_{1.8}Pb_{0.2}$ sample (Fig. 4). The raw Hall resistivity values ρ_H are linear with the field, with negative slopes for both samples. To further eliminate the effect of possible misalignment of the Hall electrodes, the Hall coefficient R_H was taken as $R_H = [R_H(5\text{ T}) + R_H(-5\text{ T})]/2$ at each temperature. The inset of Fig. 4 shows the Hall coefficient of $PdBi_2$ from 6 to 300 K. The Hall coefficient is negative over the whole temperature range and only weakly depends on temperature, suggesting that electron-type charge carriers dominate the charge transport. The value of the Hall coefficient changes by <30% from 2 to 300 K, implying relatively minor multiband effects, and therefore it is reasonable to evaluate the carrier concentration using the Hall coefficient R_H.

The Hall resistivities of the parent compound and the Pb-doped sample under different magnetic fields at 10 K are shown in Fig. 4, where one can see that the contribution

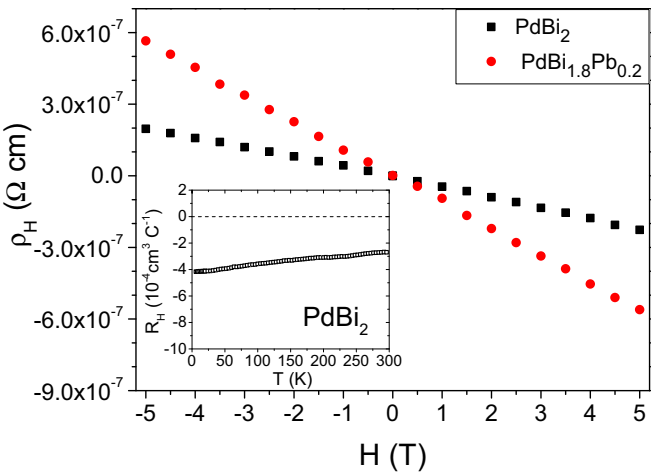

FIG. 4. (Color online) Hall resistivity of β-$PdBi_2$ and $PdBi_{1.8}Pb_{0.2}$ under a magnetic field at 10 K; the inset shows the Hall coefficient R_H of β-$PdBi_2$ from 6 to 300 K.

from magnetoresistance is rather small. The Hall coefficients R_H, determined by the slopes of the curves, are $R_H = -4.24 \times 10^{-4}$ cm^3/C and $R_H = -1.12 \times 10^{-3}$ cm^3/C for $PdBi_2$ and $PdBi_{1.8}Pb_{0.2}$, respectively. The negative Hall cofficient of the Pb-doped sample indicates that the charge carriers are still dominated by electrons. By simply using the single-band expression $n = 1/R_H q$, we can calculate the electron concentrations: $n = 1.47 \times 10^{22}$ cm^{-3} for $PdBi_2$ and $n = 5.56 \times 10^{21}$ cm^{-3} for $PdBi_{1.8}Pb_{0.2}$. The substantial decrease of electron concentration suggests effective hole doping in the $PdBi_2$ system through Pb substitution at the Bi site. This effective hole doping might shift the Fermi level, resulting in a lower electronic density of states. Therefore, the lower DOS might contribute to the decrease of T_c if a rigid-band model is adopted.

Since the hole doping by Pb substitution caused decrease of T_c, we also attempted to carry out Na intercalation, which would introduce electrons into the system. Several trials with nominal Na concentration ranging from $x = 0.1$ to $x = 0.4$ on Na_xPdBi_2 were made. X-ray powder diffraction analysis on the resulting bulk materials reveals that some small impurties (less than 10% total) of NaBi and Pd exist in the sample in addition to the formation of the β tetragonal phase. We were able to isolate smaller pure crystals from the bulk samples and carried out detailed chemical analyses and physical measurements. The isolated crystals are homegeneous from WDS analysis and have all of the three elements present. However, the actual Na content is much lower than the nominal composition. Taking the nominal $x = 0.1$ as an example, the actual composition we found from the chemical analysis was Na:Pd:Bi = 0.044(3):1:2.000(5). The highest Na doping level is ~0.057(2) determined from the chemical analysis, indicating the relatively low limit of Na intercalation into this compound compared with the Pb doping. The Na-doped crystals were moderately sensitive to air/moisture as they slowly decayed when kept outside the glovebox for one day. This also implies sucesssful Na intercalation into the system. The superconducting T_c, on the other hand, is rapidly suppressed at such a low Na-doping level, changing from 5.4 K in $PdBi_2$ down to 4.1 K in $Na_{0.044}PdBi_2$, and further down to 3.9 K in $Na_{0.057}PdBi_2$, as shown in the inset of Fig. 5(a). However, this is in great conflict with the theoretical expectation [13], which suggests that such electronlike doping should shift the Fermi level toward the DOS peak, increasing the DOS at the Fermi level and thus the T_c.

To verify whether the DOS does increase through Na intercalation, a Hall measurement was carried out on the $Na_{0.057}PdBi_2$ sample to probe the change of charge carrier concentration. As for $PdBi_2$, the Hall coefficient R_H above 50 K is T insensitive for the Na-intercalated sample, as shown in Fig. 5(a). Therefore, the electron concentrations for $PdBi_2$ and $Na_{0.057}PdBi_2$ are calculated based on the R_H at 50 K as 1.58×10^{22} cm^{-3} and 3.09×10^{22} cm^{-3}, respectively. There is apparently a significant increase of the carrier concentration, which is also in line with the decrease of the room-temperature resistivity observed in Fig. 5(b). The deduced $d\rho/dT$ at 300 K decreases from 0.37 $\mu\Omega$ cm/K for $PdBi_2$ to 0.20 $\mu\Omega$ cm/K for $Na_{0.057}PdBi_2$. The Na intercalation, therefore, does introduce electrons and enhance the DOS as expected. The suppression of T_c has to be attributed to other mechanisms.

It is well known that both the competing excitations and the impurity scattering (especially pair-broken scattering) may suppress superconductivity. To explore the issue, both the magnetoresistance and the R_H are investigated (Fig. 5). The Hall coefficient R_H is enhanced almost by a factor of 3 on cooling below 50 K [Fig. 5(a)]. As demonstrated previously (Fig. 4 inset), the multiband effect has trivial interference effects on the R_H for the undoped $PbBi_2$. The unexpected enhancement of the R_H in the Na-intercalated sample can hardly be attributed to the multiband effect, but is more likely caused by certain spin-related scattering/excitations. For example, Han *et al.* have observed that the R_H of SrFeAsF significantly increased with cooling below 150–160 K with the spin-density-wave transition around 173 K [16]. Such an interpretation seems to be supported by both the resistivity and the magnetoresistivity [Fig. 5(b)] data. However, it should be noted that these are rather general characteristics of all spin ordering/excitations. For instance, an anomalous Hall effect and colossal magnetoresistance are observed in the manganites such as $La_{1-x}Ca_xMnO_3$ [17,18]. To explore the situation in $Na_{0.057}PdBi_2$, the $R(T)$ above 70 K is fitted as a quadratic function of T [the solid red line in Fig. 5(b)], where the R drop

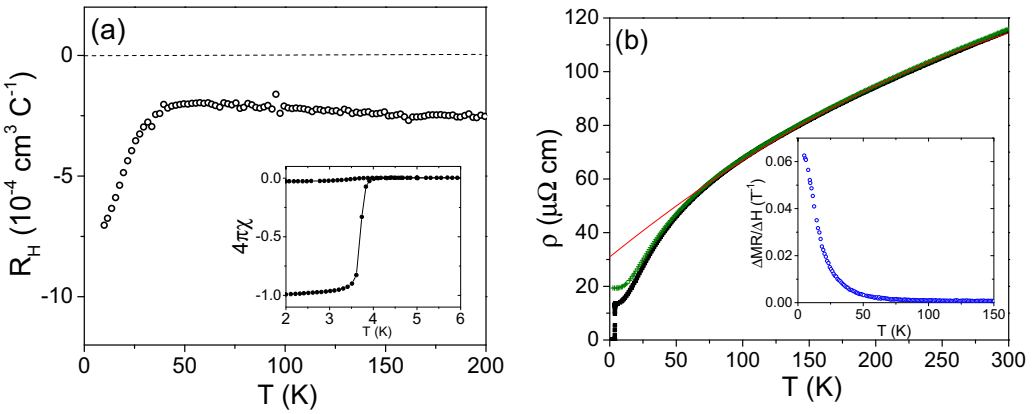

FIG. 5. (Color online) (a) The Hall coefficient R_H of $Na_{0.057}PdBi_2$ from 5 to 300 K; the inset shows the magnetic susceptibility of $Na_{0.057}PdBi_2$. (b) Magnetoresistivity of $Na_{0.057}PdBi_2$ from 2 to 300 K (solid black squares, zero field; green crosses, 7 T); The solid red line is only a guide for the eyes. The inset is the ratio of the change in the magnetoresistance $[\rho(7\text{ T}) - \rho(0\text{ T})]/\rho(0\text{ T})$ to the magnetic field.

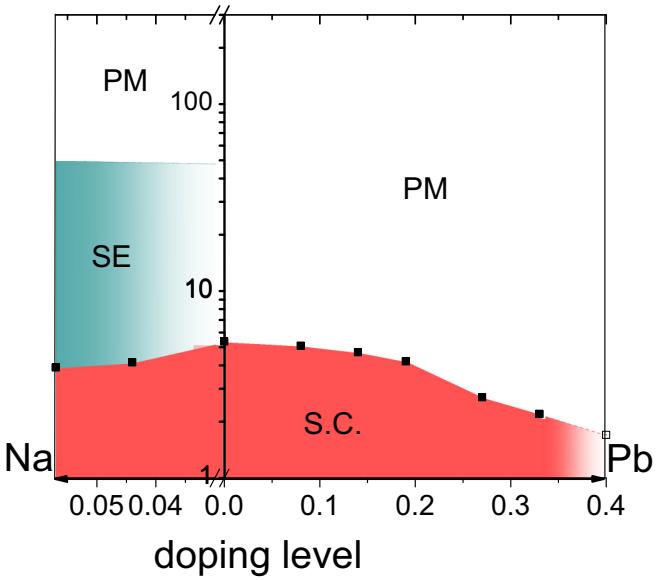

FIG. 6. (Color online) The phase diagram for both hole- and electron-doped $PdBi_2$. SC, superconducting transition temperature determined resistively; PM, paramagnetic state; "SE," possible spin excitation induced by Na intercalation.

below 50 K is evident. The $R(T)$ under a magnetic field of 7 T, in particular, is much higher than that under 0 T [Fig. 5(b) inset] with the deduced $\partial \ln R/\partial H \approx 0.05/T$ at 10 K. The enhanced hump feature, the large magnetoresistance, and the increased amplitude of the Hall coefficient below 50 K suggest a Fermi surface reconstruction and excitation/ordering in the spin section around 50 K induced by Na doping. Thus the suppressed superconductivity in Na-intercalated $PdBi_2$ could be attributed to the competing spin excitation associated with the Fermi surface reconstruction, although the exact nature of this spin excitation needs further investigation.

Based on the above data, we were able to construct the phase diagram of T_c as a function of doping level (both hole and electron doping) as shown in Fig. 6. At the right side of the phase diagram (hole doping), the T_c decreases continuously with Pb doping. The suppression of T_c can be understood as a decrease of the DOS at the Fermi level caused by hole doping. At the left side of the figure, we demonstrate that the T_c is also quickly suppressed by a small amount of Na interclation. The cause of this T_c suppression might be attributed to the emergence of possible spin exciation, which may compete for the ground state and be counterproductive in stabilizing the superconducting state.

To further examine the above conjectures based on doping, we investigated the pressure effect on the undoped $PbBi_2$ with the highest T_c of this series by measuring the temperature dependence of resistivity under pressures up to 16.63 kbar, as shown in Fig. 7. As the applied pressure increases, the normal-state resistivity considerably decreases. A closer look at the low temperature part, as shown in Fig. 7(b), reveals that the superconducting transition becomes slightly sharper, and is gradually suppressed, upon applying pressure at a linear suppression rate of $dT_c/dP = -0.28$ K/GPa. At 16.63 kbar, the T_c is reduced to 4.9 K. To verify the stability of the sample, the pressure cell was unloaded to lower pressure and ambient pressure. The corresponding data are denoted as (u) in Fig. 7(b). We observed that superconducting transition T_c values measured upon loading and unloading the pressure cell fell along the same line, proving the stability of the sample in the pressure cycle. The corresponding phase diagram of T_c versus pressure is shown in the inset of Fig. 7(b). The suppression of T_c by pressure appears to be consistent with the doping experiment.

IV. CONCLUSIONS

In summary, we have systematically grown large single crystals of the layered compounds β-$PdBi_2$, the hole-doped $PdBi_{2-x}Pb_x$, and the electron-doped Na_xPdBi_2, and studied their magnetic and transport properties. Hall measurements on $PdBi_2$, $PdBi_{1.8}Pb_{0.2}$, and $Na_{0.057}PdBi_2$ show that the charge transport is dominated by electrons in all of the samples. The electron concentration is substantially reduced upon Pb doping in $PdBi_{2-x}Pb_x$ and increased upon Na intercalation in Na_xPdBi_2, indicating effective hole doping by Pb and electron doping by Na. In Pb-doped $PdBi_2$, we observed a monotonic decrease of T_c from 5.4 K in undoped $PdBi_2$ to

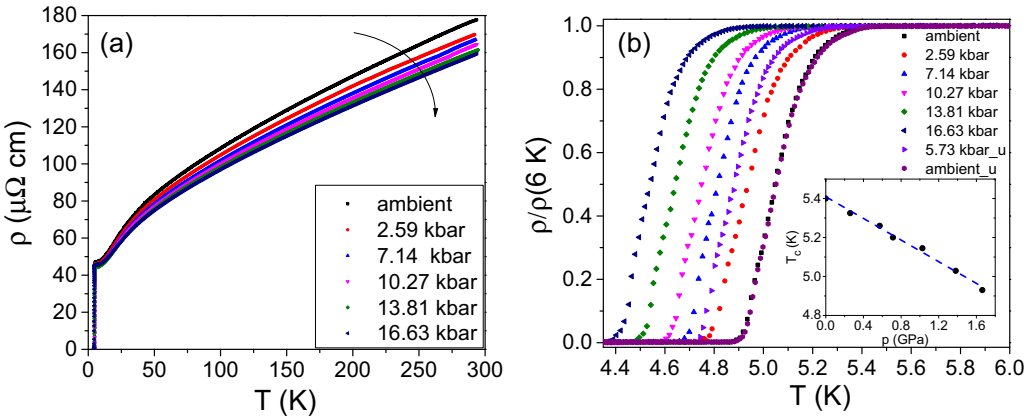

FIG. 7. (Color online) (a) The resistivity of β-$PdBi_2$ from 1.2 to 300 K under high pressure. (b) The normalized resistivity under different pressures, where u denotes the unloaded pressure run. The inset shows the shift of T_c with pressure for β-$PdBi_2$.

less than 2 K for $x > 0.35$. The monotonic decrease of the T_c upon doping can be explained by the reduced DOS at the Fermi level. In Na-intercalated samples, a rapid decrease of T_c with a slight Na-intercalation level is also observed, which is in contradiction with the theoretical expectation. Both the magnetoresistance and Hall measurements further reveal evidence for a possible competing spin excitation at ~50 K, which could contribute to the suppression of the T_c in Na-intercalated samples. Meanwhile, application of external pressure up to 16.63 kbar on the undoped $PdBi_2$ also suppresses the superconducting transition linearly with a dT_c/dP coefficient of -0.28 K/GPa, consistent with the doping experiments.

ACKNOWLEDGMENTS

The work in Houston, Texas, is supported, in part, by U.S. Air Force Office of Scientific Research Grant No. FA9550-09-1-0656, the T.L.L. Temple Foundation, the John J. and Rebecca Moores Endowment, and the State of Texas through the Texas Center for Superconductivity at the University of Houston.

[1] J. A. Wilson, F. J. Di Salvo, and S. Mahajan, Adv. Phys. **24**, 117 (1975).
[2] G. Grüner, Rev. Mod. Phys. **60**, 1129 (1988).
[3] C. dela Cruz, Q. Huang, J. W. Lynn, J. Li, W. Ratcliff, J. L. Zarestky, H. A. Mook, G. F. Chen, J. L. Luo, N. L. Wang, and P. C. Dai, Nature (London) **453**, 899 (2008).
[4] X. F. Wang, T. Wu, G. Wu, H. Chen, Y. L. Xie, J. J. Ying, Y. J. Yan, R. H. Liu, and X. H. Chen, Phys. Rev. Lett. **102**, 117005 (2009).
[5] H. Zhang, C. X. Liu, X. L. Qi, X. Dai, Z. Fang, and S. C. Zhang, Nat. Phys. **5**, 438 (2009).
[6] Y. Zhang, K. He, C. Z. Chang, C. L. Song, L. L. Wang, X. Chen, J. F. Jia, Z. Fang, X. Dai, W. Y. Shan, S. Q. Shen, Q. Niu, X. L. Qi, S. C. Zhang, X. C. Ma, and Q. K. Xue, Nat. Phys. **6**, 584 (2010).
[7] J. Nagamatsu, N. Nakagawa, T. Muranaka, Y. Zenitani, and J. Akimitsu, Nature (London) **410**, 63 (2001).
[8] S. Yamanaka, H. Kawaji, K. Hotehama, and M. Ohashi, Adv. Mater. **8**, 771 (1996).
[9] N. N. Zhuravlev, Zh. Eksp. Teor. Fiz. **32**, 1305 (1957).
[10] H. Okamoto, J. Phase Equilib. **15**, 191 (1994).
[11] B. T. Matthias, T. H. Geballe, and V. B. Compton, Rev. Mod. Phys. **35**, 1 (1963).
[12] Y. Imai, F. Nabeshima, T. Yoshinaka, K. Miyatani, R. Kondo, S. Komiya, I. Tsukada, and A. Maeda, J. Phys. Soc. Jpn. **81**, 113708 (2012).
[13] E. Herrera, I. Guillamon, J. A. Galvis, A. Correa, A. Fente, R. F. Luccas, F. J. Mompean, M. García-Hernández, S. Vieira, J. P. Brison and H. Suderow, Phys. Rev. B **92**, 054507 (2015).
[14] I. R. Shein and A. L. Ivanovskii, J. Supercond. Novel Magn. **26**, 1 (2013).
[15] C. W. Chu, Phys. Rev. Lett. **33**, 1283 (1974).
[16] F. Han, X. Zhu, G. Mu, P. Cheng, and H. H. Wen, Phys. Rev. B **78**, 180503 (2008).
[17] P. Schiffer, A. P. Ramirez, W. Bao, and S-W. Cheong, Phys. Rev. Lett. **75**, 3336 (1995).
[18] P. Matl, N. P. Ong, Y. F. Yan, Y. Q. Li, D. Studebaker, T. Baum, and G. Doubinina, Phys. Rev. B **57**, 10248 (1998).